

Masakazu Sugishima,^a Norihiko Tanimoto,^a Koji Soda,^{b,c} Norio Hamada,^{b,c} Fumio Tokunaga^{b,c} and Keiichi Fukuyama^{a*}

^aDepartment of Biology, Graduate School of Science, Osaka University, Machikaneyama-cho 1-1, Toyonaka, Osaka 560-0043, Japan,

^bDepartment of Earth and Space Science, Graduate School of Science, Osaka University, Machikaneyama-cho 1-1, Toyonaka, Osaka 560-0043, Japan, and ^cJST-CREST, 2-1 Yamadaoka, Suita, Osaka 565-0871, Japan

Correspondence e-mail:

fukuyama@bio.sci.osaka-u.ac.jp

Structure of photoactive yellow protein (PYP) E46Q mutant at 1.2 Å resolution suggests how Glu46 controls the spectroscopic and kinetic characteristics of PYP

Photoactive yellow protein from *Ectothiorhodospira halophila* is a photoreceptor protein involved in the negative phototaxis of this bacterium. Its chromophore (*p*-coumaric acid) is deprotonated in the ground state, which is stabilized by a hydrogen-bond network between Tyr42, Glu46 and Thr50. Glu46 is a key residue as it has been suggested that the proton at Glu46 is transferred to the chromophore during its photoconversion from the dark state to the signalling state. The structure of E46Q mutant protein was determined at 1.2 Å resolution, revealing that the phenolic O atom of *p*-coumaric acid is hydrogen bonded to NH₂ of Gln46 in E46Q with a longer distance (2.86 ± 0.02 Å) than its distance (2.51 Å) to Glu46 OH in the wild type. This and the decreased thermal stability of E46Q relative to the wild type show that this hydrogen bond is weakened in the E46Q mutant compared with the corresponding bond in the wild type. Several characteristic features of E46Q such as an alkali shift in the pK_a and the rapid photocycle can be explained by this weakened hydrogen bond. Furthermore, the red shift in the absorption maximum in E46Q can be explained by the delocalization of the electron on the phenolic oxygen of *p*-coumaric acid owing to the weakening of this hydrogen bond.

1. Introduction

Photoactive yellow protein (PYP) from *Ectothiorhodospira halophila* is a small (14 kDa) water-soluble protein and a blue-light photoreceptor (Meyer, 1985) that is implicated in the negative phototaxis of the bacterium (Sprenger *et al.*, 1993). PYP is the structural prototype for a large and diverse family of sensory and signalling proteins containing the PAS-sequence motif (Pellequer *et al.*, 1998). X-ray crystallography has revealed that PYP has an α/β -fold structure characterized by a central twisted six-stranded antiparallel β -sheet flanked by loops and helices (Borgstahl *et al.*, 1995; Genick *et al.*, 1998). One side of the β -sheet has an N-terminal loop structure and the other side has a loop containing Cys69, which is linked to the chromophore, *p*-coumaric acid, by a thioester bond. The anionic *trans*-type chromophore (Hoff *et al.*, 1994; Baca *et al.*, 1994) is buried within a hydrophobic core and forms a hydrogen-bonding network with Glu46, Tyr42 and Thr50 (Borgstahl *et al.*, 1995; Genick *et al.*, 1998).

On light absorption, PYP undergoes a photocycle containing several intermediates that is closely linked to the function of the protein (Meyer *et al.*, 1987; Kort *et al.*, 1996; Imamoto *et al.*, 1996). Several reports have shown the possibility that a proton is transferred between the chromophore and Glu46 in this cycle (Xie *et al.*, 1996, 2001; Imamoto *et al.*, 1997). Consequently, Glu46 is an important residue in PYP and extensive research focused on Glu46 has been performed

Received 17 March 2004

Accepted 24 September 2004

PDB Reference: photoactive yellow protein E46Q mutant, 1ugu, r1uguf.

using the mutant E46Q (Genick *et al.*, 1997; Devanathan *et al.*, 1999; Zhou *et al.*, 2001; Imamoto *et al.*, 2001; Borucki *et al.*, 2002, 2003; Meyer *et al.*, 2003; Derix *et al.*, 2003). The E46Q mutant has an absorption maximum at 460 nm, which is greatly red-shifted from the 446 nm absorption maximum of the wild type (WT; Mihara *et al.*, 1997). The pK_a of E46Q is 5.3 compared with 2.8 for WT and the photocycle of E46Q is faster than that of WT (Imamoto *et al.*, 2001; Genick *et al.*, 1997). Recently, NMR analysis has shown that there is less photoinduced structural change in E46Q than in WT (Derix *et al.*, 2003). Thus, it is necessary to determine exactly how the structure is perturbed by the replacement of glutamic acid at residue 46 by glutamine.

In order to provide a structural basis for the characteristic features of the E46Q mutant protein and to further elucidate the role of Glu46, we determined the structure of the mutant protein in the ground state by X-ray crystallographic analysis. This paper reports the E46Q mutant structure in space group $P6_5$ at 1.20 Å resolution and provides an explanation for the difference in spectral and kinetic features between the E46Q mutant and wild-type proteins.

2. Material and methods

2.1. Preparation and crystallization of PYP E46Q mutant

The E46Q mutant of PYP was prepared as described previously (Mihara *et al.*, 1997; Imamoto *et al.*, 1995). The E46Q mutant of PYP was crystallized under conditions similar to those used for crystallization of WT PYP in space group $P6_5$ (Borgstahl *et al.*, 1995; Genick *et al.*, 1998); the solution contained poly(ethyleneglycol) monomethylether (MW 2000) and 2-(*N*-morpholino)ethanesulfonic acid pH 6.5. Hexagonal crystals appeared in 1 d.

2.2. Data collection and structure determination

The crystal was mounted in a cryoloop and flash-cooled in a nitrogen-gas stream at 100 K. Diffraction data were collected using synchrotron radiation ($\lambda = 0.650$ Å) at beamline BL41XU, SPring-8 with a MAR CCD detector. The distance between the crystal and the CCD was 130 mm. To cover a wide range of diffraction intensities, two data sets were obtained from one crystal over a total oscillation angle of 135° ; one was obtained by oscillating the crystal by 0.5° per frame and the other by 3.0° per frame with an attenuated X-ray dose. These diffraction data were processed, merged and scaled with *HKL2000* (Otwinowski & Minor, 1997). Crystallographic data and diffraction statistics are shown in Table 1.

The PYP E46Q mutant structure was solved by molecular replacement using the program *CNS* (Brünger *et al.*, 1998) using PYP in space group $P6_3$ (Borgstahl *et al.*, 1995) as a search model, excluding the chromophore (*p*-coumaric acid). Initial refinement including water molecules as well as *p*-coumaric acid was performed with the program *CNS* using 35–2.0 Å data. Subsequent refinement incorporating anisotropic temperature factors for individual atoms was performed with the *CCP4* programs *REFMAC5* and the *CCP4* suite using

Table 1

Summary of crystallographic statistics.

Crystal system	Hexagonal
Space group	$P6_5$
Unit-cell parameters (Å)	$a = b = 40.4, c = 118.0$
No. of molecules in AU	1
Resolution range (Å)	35.0–1.20
No. of observations	277326
No. of unique reflections	31902
Redundancy	8.3
Completeness† (%)	94.5 (82.4)
Mean $I/\sigma(I)$ †	18.1 (3.4)
$R_{\text{sym}}^{\ddagger}$	0.037 (0.368)
R/R_{free}^{\S}	0.165/0.191
No. of protein atoms (mean B , Å ²)	966 (16.69)
No. of water molecules (mean B , Å ²)	180 (30.64)
No. of ligand atoms (mean B , Å ²)	11 (11.87)
R.m.s. deviations from ideality	
Bond lengths (Å)	0.011
Angles (°)	1.44
Ramachandran plot	
Most favoured (%)	90.3
Additional allowed (%)	9.7

† Values in parentheses are for the outermost shell (1.24–1.20 Å). $\ddagger R_{\text{sym}} = \sum_{hkl} \sum_i |I_i(hkl) - \langle I(hkl) \rangle| / \sum_{hkl} \sum_i I_i(hkl)$, where $\langle I(hkl) \rangle$ is the mean intensity of multiply recorded reflections. $\S R = \sum |F_{\text{obs}}(hkl) - F_{\text{calc}}(hkl)| / \sum |F_{\text{obs}}(hkl)|$. R_{free} is the R value calculated for 10% of the data set not included in the refinement.

35–1.2 Å data (Collaborative Computational Project, Number 4, 1994; Murshudov *et al.*, 1999). Bond lengths and angles for the protein as well as for *p*-coumaric acid were restrained throughout the refinement. Restraints for *p*-coumaric acid were generated from the wild-type structure in space group $P6_3$ (Borgstahl *et al.*, 1995). The orientation of the amide group of Gln46 was confirmed by $2F_o - F_c$ and $F_o - F_c$ maps assuming residue 46 to be glutamate and by subsequent refinement in which the lengths of the two C–O bonds were restrained to be identical; the bond length of the group directed towards the phenolic oxygen of *p*-coumaric acid converged to be longer than that on the other side. We performed four rounds of block-matrix least-squares refinement with the program *SHELX* in order to calculate the estimated standard uncertainties of the hydrogen-bond lengths (Sheldrick & Schneider, 1997). The PYP molecule was divided into four overlapping blocks of 35 residues each. All residues involved in the hydrogen-bonding network to the chromophore were included in a single block. Refinement statistics are given in Table 1.

2.3. Measurements of the thermostability of PYP and its E46Q mutant

PYP and the E46Q mutant were each dissolved in 10 mM 3-morpholinopropanesulfonic acid pH 7.5. The absorption spectra of both proteins were measured in the temperature range 283–363 K with an interval of 5 K. The samples were incubated at each temperature for 5 min and their absorption spectra were measured when the fluctuation in the temperature became less than 0.1 K. Jasco ETC-505S and ETC-505T temperature controllers were used for thermal control and the spectra were recorded with a Jasco V-530 UV–Vis spectrophotometer. The spectra of PYP and its E46Q mutant in the range 283–353 K showed isosbestic points (387 nm for WT,

390 nm for the E46Q mutant), indicating that the denaturations of PYP and its E46Q mutant are transitions between two species, native and denatured states. The T_m temperatures of PYP and its E46Q mutant were calculated by fitting the experimental data to a two-state transition model.

3. Results and discussion

The PYP E46Q mutant structure was refined at 1.2 Å resolution to final R and R_{free} factors of 0.165 and 0.192, respectively. The overall structure of the PYP E46Q mutant is very similar to the WT PYP structure in space group $P6_5$ (van Aalten *et al.*, 2000), whereas residues 114–116 are additionally ordered. The root-mean-square deviation of main-chain atoms between the E46Q mutant and WT is 0.54 Å. This is consistent with the recent NMR analysis of the E46Q mutant in the ground state (Derix *et al.*, 2003). The structural differences observed between the WT structures in space groups $P6_5$ and $P6_3$ (van Aalten *et al.*, 2000) are conserved in the E46Q mutants of space groups $P6_5$ and $P6_3$ (Anderson *et al.*, 2004). The side-chain orientation of Gln46 is key to understanding how the electronic absorption of the mutant has been red-shifted, as the protonation state of the phenol group of *p*-coumaric acid is the primary factor for PYP colour and regulates the photocycle rate. *p*-Coumaric acid is deprotonated in PYP and its absorption maximum ($\lambda_{\text{max}} = 446$ nm) is markedly red-shifted compared with that in the protonated state ($\lambda_{\text{max}} \approx 360$ nm). The hydrogen bond from residue 46 to *p*-coumaric acid stabilizes the deprotonated state of the phenolic oxygen of *p*-coumaric acid. The shape of the $2F_o - F_c$ map of residue 46 indicates that the amide N atom of Gln46 is directed towards *p*-coumaric acid and can hydrogen bond to it (Fig. 1*a*). Whether it is the O or N atom of the amide group of

Gln46 that is directed towards the phenolic oxygen of *p*-coumaric acid was determined by inspection of the $F_o - F_c$ map calculated assuming residue 46 to be glutamate; negative density should appear in the $F_o - F_c$ map for the C–N bond in the E46Q mutant as the C–N bond is longer than the C=O bond. Negative density appeared for the bond whose terminal atom is close to the phenolic oxygen of *p*-coumaric acid (Fig. 1*a*). This clearly shows that the amide nitrogen of Gln46 is hydrogen bonded to *p*-coumaric acid.

Superimposition of the E46Q mutant on $P6_5$ WT PYP is shown in Fig. 1(*b*), which indicates that the conformations of the side chains around *p*-coumaric acid are generally conserved in the E46Q mutant, but that the phenol group of *p*-coumaric acid slightly changes its position. The length of the hydrogen bond between *p*-coumaric acid and Gln46 changes from 2.51 Å in WT to 2.86 ± 0.02 Å in E46Q, while retaining the hydrogen-bonding scheme between the phenolic oxygen of *p*-coumaric acid, Tyr42 and Gln46. On the other hand, the distance between the phenolic oxygen of the chromophore and Tyr42 in E46Q is nearly identical to that in WT [2.50 Å in WT (PDB code 1d7e), 2.48 ± 0.02 Å in the E46Q mutant] and the chromophore of E46Q is tilted a little relative to that in WT. These results are consistent with the very recent crystallographic results on the PYP E46Q mutant in space groups $P6_3$ and $P6_5$ (Anderson *et al.*, 2004). In addition, the length of the hydrogen bond between the carbonyl O atom of the chromophore and the amide group of Cys69 in E46Q is slightly longer than that in WT (E46Q, 2.90 ± 0.02 Å; WT, 2.81 Å).

The features of the E46Q mutant can be summarized in three points: a red shift in the absorption spectrum, a pK_a shift to the alkali side and a more rapid reaction rate (Genick *et al.*, 1997). This crystallographic structure analysis revealed that a

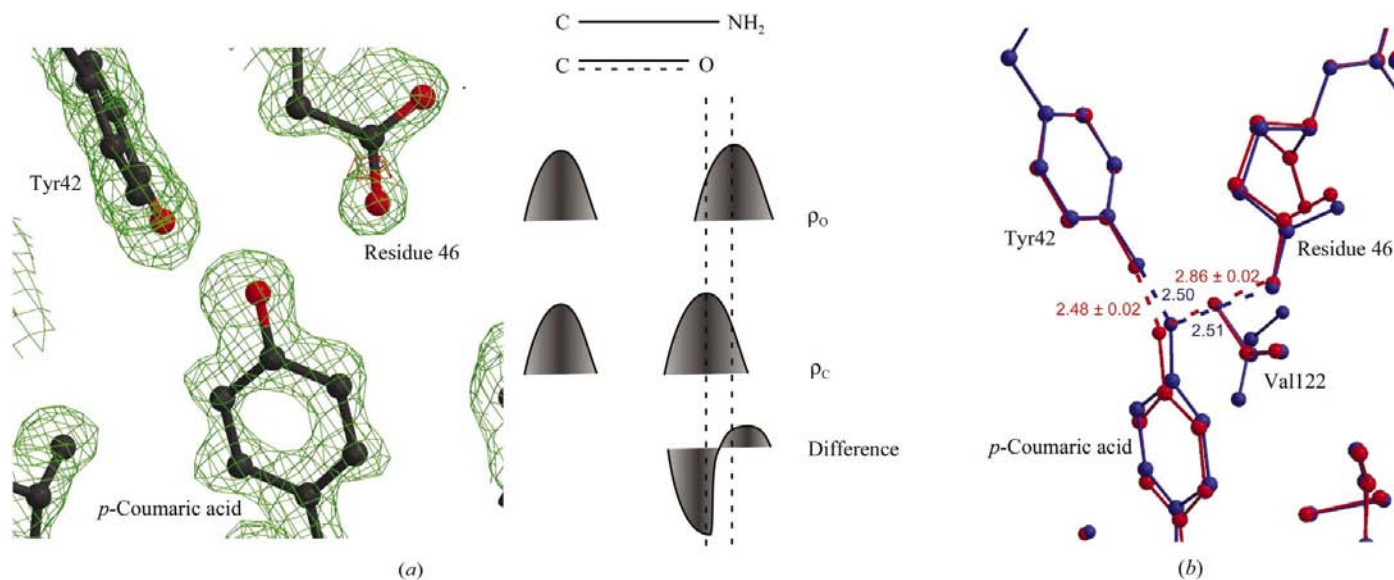


Figure 1

(*a*) Electron density around *p*-coumaric acid. A σ_A -weighted $2F_o - F_c$ map, omitting *p*-coumaric acid, Gln46 and Tyr42 and contoured at 1.5σ (green), was superimposed on the ball-and-stick model of PYP. An $F_o - F_c$ map contoured at -3.0σ (red) was also superimposed on the model. The $F_o - F_c$ map was calculated assuming residue 46 to be glutamate. (*b*) Superimposition of the E46Q mutant on WT PYP. A wire-frame model of the E46Q mutant (red) was superimposed on that of WT PYP, space group $P6_5$ (PDB code 1d7e). Dashed lines indicate the hydrogen bonds of the phenolic oxygen of *p*-coumaric acid. Numerals show the lengths of these hydrogen bonds in Å.

small but significant structural change has occurred around the chromophore on replacement of Glu46 by Gln, without a change in the overall structure. This indicates that this small spatial change as well as the different functional group (the amide group of Gln and the hydroxide group of Glu) cause these distinct features of the E46Q mutant. The phenolic oxygen is deprotonated in the E46Q mutant at neutral pH and the localization of electrons at the phenolic oxygen may be affected by the hydrogen bonds from residue 46 and Tyr42 to the phenolic oxygen. The crystal structure revealed that the NH₂ group faces the phenolic group of the chromophore. The

distance between the amide N atom of Gln46 and the phenolic oxygen of the chromophore is $2.86 \pm 0.02 \text{ \AA}$ and is longer than the distance between the carbonyl O atom of Glu46 and the phenolic oxygen of the chromophore (2.51 \AA) in WT. Considering the basicity of these groups, the hydrogen bond between the chromophore and residue 46 in the E46Q mutant is expected to be weaker than that in WT. It has been noted that short hydrogen bonds are stronger than ordinary hydrogen bonds, but the magnitude of the additional stabilization gained by short hydrogen bonds in proteins and protein complexes is under debate (Poi *et al.*, 2003; Usher *et al.*, 1994). The decreased thermal stability of E46Q mutant ($T_m = 345.5 \pm 0.5 \text{ K}$, $N = 6$) compared with that of WT ($T_m = 354.1 \pm 0.7 \text{ K}$, $N = 3$) (Fig. 2) supports the weakening of the hydrogen bond concerned. The pK_a shift to the alkali side in the E46Q mutant is consistent with the weakened hydrogen bond between the amide group of Gln46 and the phenolic oxygen because the protonation of the chromophore caused by an increase in acidity accompanies a partial unfolding that would rearrange or disrupt the hydrogen-bond network (Hoff *et al.*, 1997). The weakening of this hydrogen bond in the E46Q mutant shown by this analysis suggests that delocalization of the electron on the phenolic oxygen of the chromophore is induced (Fig. 3). Quantum-chemical analysis of the model compounds of PYP has shown that the hydrogen-bond network composed of Tyr42, Glu46 and Thr50 localizes the electron on the phenolic O atom of *p*-coumaric acid and blue-shifts the absorption maximum of the chromophore (Yoda *et al.*, 2001). Thus, substitution of Glu46 by Gln would contribute to delocalization of the electron on the phenolic oxygen and lower the blue-shift effect. A red shift of the absorption maximum and an alkali shift in pK_a are observed in Y42F and T50V mutants in which part of this hydrogen-bond network is disrupted (Brudler *et al.*, 2000).

On the other hand, in the step in the photocycle of PYP from the M intermediate ($\lambda_{max} = 355 \text{ nm}$; the chromophore is protonated) to the ground state ($\lambda_{max} = 446 \text{ nm}$; the chromophore is deprotonated) deprotonation and a *cis/trans* transition of the chromophore take place. Therefore, the hydrogen-bond strength between *p*-coumaric acid and residue 46 is also related to the reaction rate of PYP. A weakened hydrogen bond may loosen the restraint of keeping the photoactivated *p*-coumaric acid in the *trans* form and accelerate the formation of the M intermediate. Such a smooth transition to the M intermediate in the E46Q mutant may prevent partial unfolding in the M intermediate (Derix *et al.*, 2003) and promote the transition from the M intermediate to ground state. This may be one reason for the acceleration of the photocycle.

Note added in proof. After submission of this manuscript, the crystal structures of PYP E46Q mutant in space group $P6_5$ at 1.40 \AA resolution and in space group $P6_3$ at 0.95 \AA resolution were reported (Anderson *et al.*, 2004). Because the structure of PYP, especially around Asp20, Lys80 and Met100, is slightly changed by crystallization artefacts (van Aalten *et al.*, 2000), accurate structures in space groups $P6_5$ and $P6_3$ are desirable to discuss the chemical features of PYP. The reso-

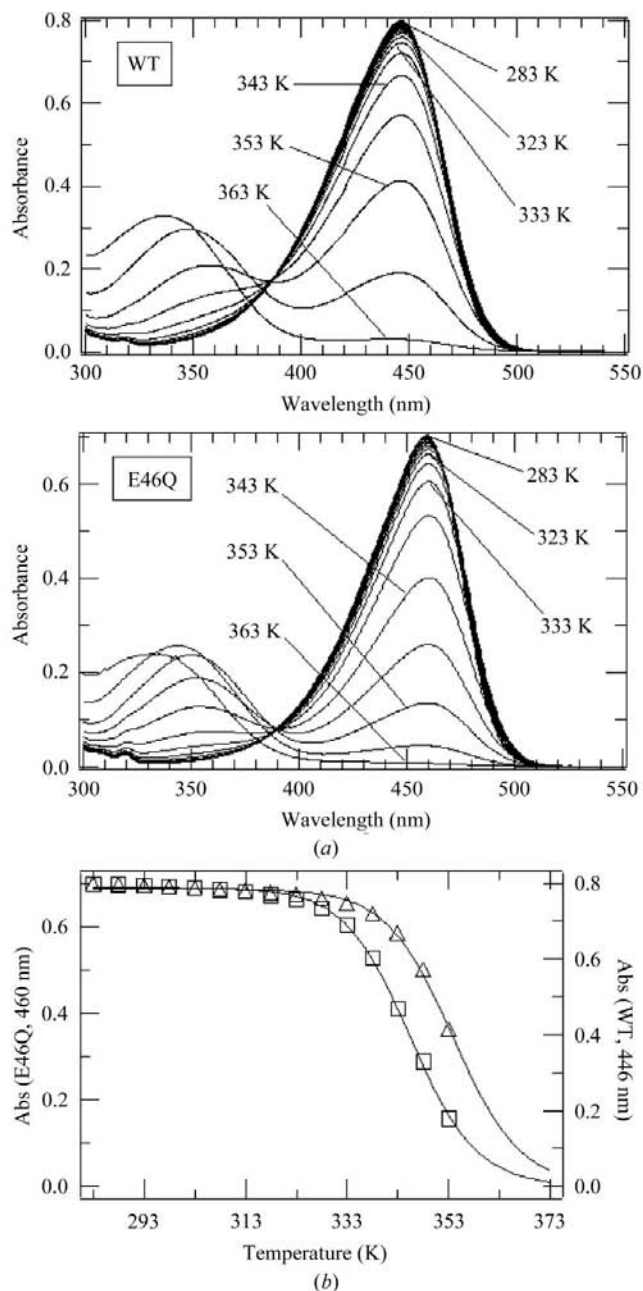


Figure 2 Temperature-dependence of the UV-visible absorption spectra of E46Q. (a) The absorption spectra of WT and E46Q at the following temperatures: 283, 288, 293, 298, 303, 308, 313, 318, 323, 328, 333, 338, 343, 348, 353, 358 and 363 K. (b) The absorbance changes of WT (triangles) and E46Q (squares).

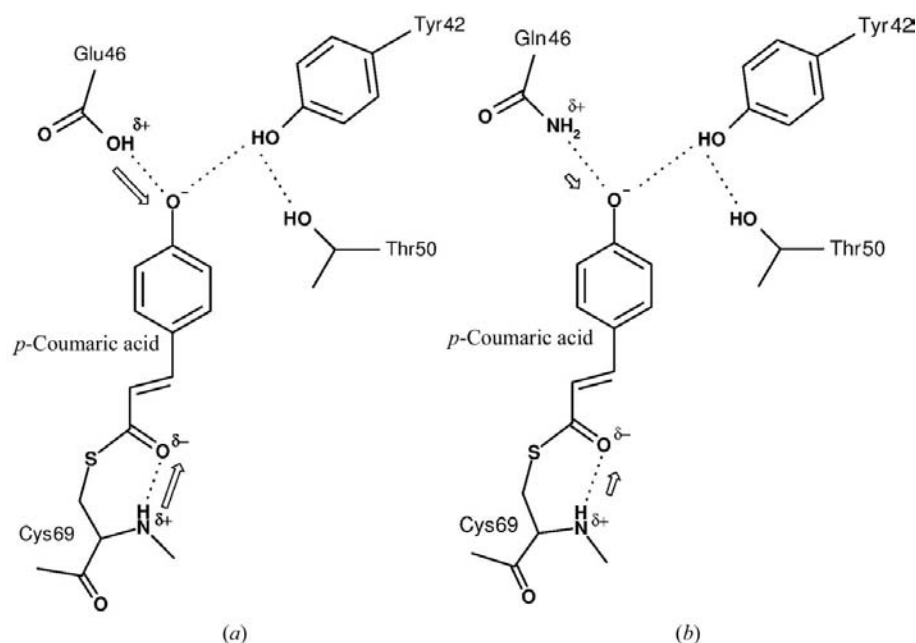


Figure 3
Schematic diagram of *p*-coumaric acid and residues around the chromophore in (a) WT and (b) the E46Q mutant. Open arrows represent the localization of electrons of *p*-coumaric acid.

lution of the diffraction data used to refine the structure in *P6₅* space group by us is higher than that by Anderson *et al.* (2004). In addition, PYP has fewer intermolecular contacts in space group *P6₅* than in space group *P6₃*, indicating that the structure in space group *P6₅* may be less affected by crystal-packing artefacts (van Aalten *et al.*, 2000).

We thank Drs Masahide Kawamoto and Hisanobu Sakai for their kind help with data collection using synchrotron radiation at BL41XU, SPring-8. This work was supported by CREST of Japan Science and Technology Association to FT and by a Grant-in-Aid for Scientific Research (C) 14580674 to KF from the Ministry of Education, Culture, Sports, Science and Technology of Japan.

References

Aalten, D. M. van, Crielgaard, W., Hellingwerf, K. J. & Joshua-Tor, L. (2000). *Protein Sci.* **9**, 64–72.
 Anderson, S., Crosson, S. & Moffat, K. (2004). *Acta Cryst.* **D60**, 1008–1016.
 Baca, M., Borgstahl, G. E., Boissinot, M., Burke, P. M., Williams, D. R., Slater, K. A. & Getzoff, E. D. (1994). *Biochemistry*, **33**, 14369–14377.
 Borgstahl, G. E., Williams, D. R. & Getzoff, E. D. (1995). *Biochemistry*, **34**, 6278–6287.
 Borucki, B., Devanathan, S., Otto, H., Cusanovich, M. A., Tollin, G. & Heyn, M. P. (2002). *Biochemistry*, **41**, 10026–10037.
 Borucki, B., Otto, H., Joshi, C. P., Gasperi, C., Cusanovich, M. A., Devanathan, S., Tollin, G. & Heyn, M. P. (2003). *Biochemistry*, **42**, 8780–8790.
 Brudler, R., Meyer, T. E., Genick, U. K., Devanathan, S., Woo, T. T., Millar, D. P., Gerwert, K., Cusanovich, M. A., Tollin, G. & Getzoff, E. D. (2000). *Biochemistry*, **39**, 13478–13486.
 Brünger, A. T., Adams, P. D., Clore, G. M., DeLano, W. L., Gros, P., Grosse-Kunstleve, R. W., Jiang, J.-S., Kuszewski, J., Nilges, M.,

Pannu, N. S., Read, R. J., Rice, L. M., Simonson, T. & Warren, G. L. (1998). *Acta Cryst.* **D54**, 905–921.
 Collaborative Computational Project, Number 4 (1994). *Acta Cryst.* **D50**, 760–763.
 Derix, N. M., Wechselberger, R. W., van der Horst, M. A., Hellingwerf, K. J., Boelens, R., Kaptein, R. & van Nuland, N. A. J. (2003). *Biochemistry*, **42**, 14501–14506.
 Devanathan, S., Brudler, R., Hessler, B., Woo, T. T., Gerwert, K., Getzoff, E. D., Cusanovich, M. A. & Tollin, G. (1999). *Biochemistry*, **38**, 13766–13772.
 Genick, U. K., Devanathan, S., Meyer, T. E., Canestrelli, I. L., Williams, E., Cusanovich, M. A., Tollin, G. & Getzoff, E. D. (1997). *Biochemistry*, **36**, 8–14.
 Genick, U. K., Soltis, S. M., Kuhn, P., Canestrelli, I. L. & Getzoff, E. D. (1998). *Nature (London)*, **392**, 206–209.
 Hoff, W. D., Dux, P., Hard, K., Devreese, B., Nugteren-Roodzant, I. M., Crielgaard, W., Boelens, R., Kaptein, R., van Beeumen, J. & Hellingwerf, K. J. (1994). *Biochemistry*, **33**, 13959–13962.
 Hoff, W. D., van Stokkum, I. H. M., Gural, J. & Hellingwerf, K. J. (1997). *Biochim. Biophys. Acta*, **1322**, 151–162.
 Imamoto, Y., Ito, T., Kataoka, M. & Tokunaga, F. (1995). *FEBS Lett.* **374**, 157–160.
 Imamoto, Y., Kataoka, M. & Tokunaga, F. (1996). *Biochemistry*, **35**, 14047–14053.
 Imamoto, Y., Koshimizu, H., Mihara, K., Hisatomi, O., Mizukami, T., Tsujimoto, K., Kataoka, M. & Tokunaga, F. (2001). *Biochemistry*, **40**, 4679–4685.
 Imamoto, Y., Mihara, K., Hisatomi, O., Kataoka, M., Tokunaga, F., Bojkova, N. & Yoshihara, K. (1997). *J. Biol. Chem.* **272**, 12905–12908.
 Kort, R., Vonk, H., Xu, X., Hoff, W. D., Crielgaard, W. D. & Hellingwerf, K. J. (1996). *FEBS Lett.* **382**, 73–78.
 Meyer, T. E. (1985). *Biochim. Biophys. Acta*, **806**, 175–183.
 Meyer, T. E., Devanathan, S., Woo, T., Getzoff, E. D., Tollin, G. & Cusanovich, M. A. (2003). *Biochemistry*, **42**, 3319–3325.
 Meyer, T. E., Yakali, E., Cusanovich, M. A. & Tollin, G. (1987). *Biochemistry*, **26**, 418–423.
 Mihara, K., Hisatomi, O., Imamoto, Y., Kataoka, M. & Tokunaga, F. (1997). *J. Biochem.* **121**, 876–880.
 Murshudov, G. N., Lebedev, A., Vagin, A. A., Wilson, K. S. & Dodson, E. J. (1999). *Acta Cryst.* **D55**, 247–255.
 Otwinowski, Z. & Minor, W. (1997). *Methods Enzymol.* **276**, 307–326.
 Pellequer, J. L., Smith, K. A. W., Kay, S. A. & Getzoff, E. D. (1998). *Proc. Natl Acad. Sci. USA*, **95**, 5884–5890.
 Poi, M. J., Tamaszewski, J. W., Yuan, C. H., Dunlap, C. A., Andersen, N. H., Gelb, M. H. & Tsai, M. D. (2003). *J. Mol. Biol.* **329**, 997–1009.
 Sheldrick, G. & Schneider, T. (1997). *Methods Enzymol.* **277**, 319–343.
 Sprenger, W. W., Hoff, W. D., Armitage, J. P. & Hellingwerf, K. J. (1993). *J. Bacteriol.* **175**, 3096–3104.
 Usher, K. C., Remington, S. J., Martin, D. P. & Drueckhammer, D. G. (1994). *Biochemistry*, **33**, 7753–7759.
 Xie, A., Hoff, W. D., Kroon, A. R. & Hellingwerf, K. J. (1996). *Biochemistry*, **35**, 14671–14678.
 Xie, A., Kelemen, L., Hendriks, J., White, B. J., Hellingwerf, K. J. & Hoff, W. D. (2001). *Biochemistry*, **40**, 1510–1517.
 Yoda, M., Houjou, H., Inoue, Y. & Sakurai, M. (2001). *J. Phys. Chem. B*, **105**, 9887–9895.
 Zhou, Y., Ujj, L., Meyer, T. E., Cusanovich, M. A. & Atkinson, G. H. (2001). *J. Phys. Chem. A*, **105**, 5719–5726.